



INSTITUT NATIONAL DE RECHERCHE EN INFORMATIQUE ET EN AUTOMATIQUE

***Incremental displacement-correction schemes for the  
explicit coupling of a thin structure with an  
incompressible fluid***

Miguel A. Fernández

**N° 7474**

December 2010

Thème BIO

**R**apport  
de recherche





## Incremental displacement-correction schemes for the explicit coupling of a thin structure with an incompressible fluid

Miguel A. Fernández\*

Thème BIO — Systèmes biologiques  
Projet REO

Rapport de recherche n° 7474 — December 2010 — 9 pages

**Abstract:** In this note we propose two incremental displacement-correction schemes for the explicit coupling of a thin structure with an incompressible fluid. The stability and the superior accuracy of these schemes (with respect to the original non-incremental variant) are theoretically analyzed and then numerically confirmed in a benchmark.

**Key-words:** Fluid-structure interaction, incremental displacement-correction, fluid incompressibility, time discretization, explicit coupling.

\* INRIA, REO project-team

## Schémas avec correction de déplacement incrémentale pour le couplage explicite d'une structure mince et d'un fluide incompressible

**Résumé :** Dans cette note nous proposons deux schémas avec correction de déplacement incrémentale pour le couplage explicite d'une structure mince et d'un fluide incompressible. La stabilité et la précision supérieure de ces schémas (par rapport à la variante originale non-incrémentale) sont analysées théoriquement et puis confirmées numériquement.

**Mots-clés :** Interaction fluide-structure, correction de déplacement incrémentale, fluide incompressible, discrétisation en temps, couplage explicite.

## Contents

<b>1</b>	<b>Introduction</b>	<b>3</b>
<b>2</b>	<b>A linear fluid-structure model problem</b>	<b>3</b>
<b>3</b>	<b>Incremental displacement-correction schemes</b>	<b>4</b>
3.1	Stability . . . . .	6
3.2	Consistency . . . . .	7
<b>4</b>	<b>Numerical experiment</b>	<b>7</b>
<b>5</b>	<b>Conclusion</b>	<b>8</b>

## 1 Introduction

The stability of numerical approximations of fluid-structure interaction problems involving an incompressible fluid and an elastic structure is very sensitive to the way the interface coupling conditions (kinematic and kinetic continuity) are treated at the discrete level. For instance, it is well known that the stability of explicit Dirichlet-Neumann coupling (or conventional *loosely coupled* schemes) is dictated by the amount of *added-mass effect* in the system (see, *e.g.*, [2]). In other words, a large fluid/solid density ratio combined with a slender and lengthy geometry gives rise to numerical instability, irrespectively of the discretization parameters. Examples in blood flows simulations are popular (see, *e.g.*, [5]). Stable explicit coupling alternatives, circumventing these infamous instabilities, have only recently been proposed in the literature. In [1], stability is achieved through an appropriate weak treatment of the interface coupling and the addition of a weakly consistent interface compressibility. For thin structural models, the explicit coupling procedure introduced in [7] combines the splitting of the time-marching in the solid with an implicit treatment of the fluid pressure and the hydrodynamic solid contributions (fully embedded into the fluid sub-step through a Robin-like boundary condition). Since the solid displacement is ignored in the fluid sub-step, this procedure can be interpreted as a *non-incremental* displacement-correction scheme (borrowing the terminology used for projection methods in fluids, see, *e.g.*, [6, Section 3]).

In this note, we propose two *incremental* displacement-correction schemes (the displacement is extrapolated in the first step and corrected in the second). We also present a general stability and consistency result which covers both the non-incremental and the incremental variants. The analysis shows, in particular, that the non-incremental scheme is expected to yield sub-optimal time-convergence in the energy norm; on the contrary, optimal accuracy is achieved with the proposed incremental schemes, without compromising stability. This enhanced accuracy is also illustrated with a numerical experiment.

## 2 A linear fluid-structure model problem

We consider a low Reynolds regime and assume that the structure undergoes infinitesimal displacements. The fluid is described by the Stokes equations in a

fixed domain  $\Omega \stackrel{\text{def}}{=} \subset \mathbb{R}^d$  ( $d = 2, 3$ ). We consider a partition  $\partial\Omega = \Gamma \cup \Sigma$  of the fluid boundary, where  $\Sigma$  stands for the fluid-structure interface. The structure is assumed to behave as a linear thin membrane represented by the  $(d-1)$ -manifold  $\Sigma$  (see, e.g., [3]). Our simplified coupled problem reads as follows: find the fluid velocity  $\mathbf{u} : \Omega^f \times \mathbb{R}^+ \rightarrow \mathbb{R}^d$ , the fluid pressure  $p : \Omega^f \times \mathbb{R}^+ \rightarrow \mathbb{R}$  and the solid normal displacement  $\eta : \Sigma \times \mathbb{R}^+ \rightarrow \mathbb{R}$  such that

$$\left\{ \begin{array}{ll} \rho^f \partial_t \mathbf{u} - \text{div} \boldsymbol{\sigma}(\mathbf{u}, p) = \mathbf{0} & \text{in } \Omega, \\ \text{div} \mathbf{u} = 0 & \text{in } \Omega, \\ \boldsymbol{\sigma}(\mathbf{u}, p) \mathbf{n} = -p_{\Gamma} \mathbf{n} & \text{on } \Gamma, \\ \mathbf{u} - (\mathbf{u} \cdot \mathbf{n}) \mathbf{n} = \mathbf{0} & \text{on } \Sigma, \\ \mathbf{u} \cdot \mathbf{n} = \dot{\eta} & \text{on } \Sigma, \end{array} \right. \quad (1)$$

$$\left\{ \begin{array}{ll} \rho^s \epsilon \partial_t \dot{\eta} + L^v \dot{\eta} + L^e \eta = -(\boldsymbol{\sigma}(\mathbf{u}, p) \mathbf{n}) \cdot \mathbf{n} & \text{in } \Sigma, \\ \dot{\eta} = \partial_t \eta & \text{in } \Sigma, \\ \eta = 0 & \text{on } \partial\Sigma, \end{array} \right.$$

complemented with the initial conditions  $\mathbf{u}(0) = \mathbf{u}_0$ ,  $\eta(0) = \eta_0$  and  $\dot{\eta}(0) = v_0$ . Here,  $\rho^f$  and  $\rho^s$  stand for the fluid and solid densities,  $\epsilon$  for the solid thickness,  $\boldsymbol{\sigma}(\mathbf{u}, p) \stackrel{\text{def}}{=} -p\mathbf{I} + 2\mu\boldsymbol{\epsilon}(\mathbf{u})$  for the fluid Cauchy stress tensor,  $\mu$  for the fluid dynamic viscosity,  $\boldsymbol{\epsilon}(\mathbf{u}) \stackrel{\text{def}}{=} \frac{1}{2}(\nabla \mathbf{u} + \nabla \mathbf{u}^T)$  for the fluid strain rate tensor,  $p_{\Gamma}$  for a given inlet/outlet pressure and  $\mathbf{n}$  for the exterior unit normal vector to  $\partial\Omega^f$ . The abstract operator  $L^e$  (resp.  $L^v$ ) describes the elastic (resp. viscoelastic) behavior of the structure.

**Remark 2.1** *Though simplified, problem (1) features some of the main stability issues that appear in complex non-linear fluid-structure interaction problems involving a viscous incompressible fluid (see, e.g., [2]).*

We assume that, for functions  $\xi \in H^1(\Sigma)$  with  $L^e \xi, L^v \xi \in L^2(\Sigma)$  and  $\zeta \in H_0^1(\Sigma)$ , the following identities hold:  $\int_{\Sigma} \zeta L^e \xi = a_e(\xi, \zeta)$  and  $\int_{\Sigma} \zeta L^v \xi = a_v(\xi, \zeta)$ ; where  $a_e$  and  $a_v$  are symmetric, continuous and non-negative bilinear forms into  $H^1(\Sigma)$ . The continuity constant of  $a_e$  is denoted by  $\beta_e$ . Problem (1) can then be rewritten in variational form as follows: for  $t > 0$ , find the fluid velocity and pressure  $(\mathbf{u}(t), p(t)) \in \mathbf{V} \times L^2(\Omega)$  and the solid displacement and velocity  $(\eta(t), \dot{\eta}(t)) \in H_0^1(\Sigma)$ , such that  $\mathbf{u} \cdot \mathbf{n}|_{\Sigma} = \dot{\eta}$ ,  $\dot{\eta} = \partial_t \eta$  and

$$\begin{aligned} \rho^f \int_{\Omega} \partial_t \mathbf{u} \cdot \mathbf{v} + \int_{\Omega} \boldsymbol{\sigma}(\mathbf{u}, p) : \boldsymbol{\epsilon}(\mathbf{v}) - \int_{\Omega} \text{div} \mathbf{u} q \\ + \rho^s \epsilon \int_{\Sigma} \partial_t \dot{\eta} \mathbf{v} \cdot \mathbf{n} + a_v(\dot{\eta}, \mathbf{v} \cdot \mathbf{n}) + a_e(\eta, \mathbf{v} \cdot \mathbf{n}) = - \int_{\Gamma} p_{\Gamma} \mathbf{v} \cdot \mathbf{n} \end{aligned} \quad (2)$$

for all  $(\mathbf{v}, q) \in \mathbf{V} \times L^2(\Omega)$  and with  $\mathbf{V} \stackrel{\text{def}}{=} \{ \mathbf{v} \in [H^1(\Omega)]^d / \mathbf{v} - (\mathbf{v} \cdot \mathbf{n}) \mathbf{n}|_{\Sigma} = \mathbf{0}, \mathbf{v} \cdot \mathbf{n}|_{\Sigma} \in H_0^1(\Sigma) \}$ .

### 3 Incremental displacement-correction schemes

In this note we address the discretization of the coupled problem (2). We consider a finite element discretization in space, using continuous piece-wise polynomial functions. For the sake of simplicity, we shall assume that the interface

$\Sigma$  is flat (see, *e.g.*, [7]). This avoids the technicalities related to the treatment of the normal vector. Let  $\mathbf{V}_h \subset \mathbf{V}$  and  $Q_h \subset H^1(\Omega)$  be the discrete spaces for the fluid velocity and pressure (the symbol  $h > 0$  denotes the maximum size of the mesh elements). The discrete space for the solid displacement and velocity is chosen as the normal-trace space  $X_h \stackrel{\text{def}}{=} \{\mathbf{v}_h \cdot \mathbf{n}|_\Sigma / \mathbf{v}_h \in \mathbf{V}_h\} \subset H_0^1(\Sigma)$ . In what follows, we shall make use of the discrete counterpart,  $L_h^e : H^1(\Sigma) \rightarrow X_h$ , of the elastic operator  $L^e$ : for  $\zeta \in H^1(\Sigma)$ ,  $L_h \zeta \in X_h$  is defined as the unique solution of  $\int_\Sigma \xi_h L_h^e \zeta = a_e(\zeta, \xi_h)$  for all  $\xi_h \in X_h$ .

**Remark 3.1** *If, in addition,  $L^e \zeta \in L^2(\Sigma)$ , we have  $\|L_h^e \zeta\|_{0,\Sigma} \leq \|L^e \zeta\|_{0,\Sigma}$ .*

---

**Algorithm 1** Incremental displacement-correction schemes:  $\eta_h^* = \eta_h^n$  or  $2\eta_h^n - \eta_h^{n-1}$ .

---

1. Fluid sub-step: find  $(\mathbf{u}_h^{n+1}, p_h^{n+1}) \in \mathbf{V}_h \times Q_h$  such that

$$\begin{cases} \rho^f \int_\Omega \partial_\tau \mathbf{u}_h^{n+1} \cdot \mathbf{v}_h + \int_\Omega \boldsymbol{\sigma}(\mathbf{u}_h^{n+1}, p_h^{n+1}) : \boldsymbol{\epsilon}(\mathbf{v}_h) - \int_\Omega \text{div} \mathbf{u}_h^{n+1} q_h \\ + a_v(\mathbf{u}_h^{n+1} \cdot \mathbf{n}, \mathbf{v}_h \cdot \mathbf{n}) + \frac{\rho^s \epsilon}{\tau} \int_\Sigma \mathbf{u}_h^{n+1} \cdot \mathbf{n} \mathbf{v}_h \cdot \mathbf{n} \\ = \frac{\rho^s \epsilon}{\tau} \int_\Sigma \dot{\eta}_h^n \mathbf{v}_h \cdot \mathbf{n} - \int_\Gamma p_\Gamma(t_{n+1}) \mathbf{v}_h \cdot \mathbf{n} - a_e(\eta_h^*, \mathbf{v}_h \cdot \mathbf{n}) \end{cases} \quad (3)$$

for all  $(\mathbf{v}_h, q_h) \in \mathbf{V}_h \times Q_h$ .

2. Solid sub-step: find  $\eta_h^{n+1} \in X_h$  and  $\dot{\eta}_h^{n+1} = \partial_\tau \eta_h^{n+1} \in X_h$  such that

$$\frac{\rho^s \epsilon}{\tau} \int_\Sigma \dot{\eta}_h^{n+1} \xi_h + a_e(\eta_h^{n+1}, \xi_h) = \frac{\rho^s \epsilon}{\tau} \int_\Sigma \mathbf{u}_h^{n+1} \cdot \mathbf{n} \xi_h + a_e(\eta_h^*, \xi_h) \quad (4)$$

for all  $\xi_h \in X_h$ .

---

The discretization in time is performed with an incremental displacement-correction scheme. These time-marching procedures split the approximation of (2) into two sequential sub-steps: the solid displacement is treated explicitly in the first and it is then corrected in the second. The proposed fully discrete schemes are detailed in Algorithm 1, where  $\tau > 0$  denotes the time-step size,  $t_n \stackrel{\text{def}}{=} n\tau$ ,  $\partial_\tau x^{n+1} \stackrel{\text{def}}{=} (x^{n+1} - x^n)/\tau$  stands for the first-order backward difference and  $\eta_h^* = \eta_h^n$  (resp.  $\eta_h^* = 2\eta_h^n - \eta_h^{n-1}$ ) is the first-order (resp. second-order) extrapolation.

The *non-incremental* scheme, that is  $\eta_h^* = 0$  in Algorithm 1, is the explicit coupling procedure recently introduced in [7]. This scheme was termed *kinematically coupled*, since it treats implicitly the hydro-dynamic fluid-solid coupling (the so-called added-mass effect) and explicitly the solid elastic stresses.

Algorithm 1 admits, in addition, an alternative interpretation as discretization of (2). Indeed, taking  $\xi_h = \mathbf{v}_h \cdot \mathbf{n}|_\Sigma$  in (4) and adding the resulting expres-

sion to (3), yields

$$\begin{aligned} & \rho^f \int_{\Omega} \partial_{\tau} \mathbf{u}_h^{n+1} \cdot \mathbf{v}_h + \int_{\Omega} \boldsymbol{\sigma}(\mathbf{u}_h^{n+1}, p_h^{n+1}) : \boldsymbol{\epsilon}(\mathbf{v}_h) - \int_{\Omega} \operatorname{div} \mathbf{u}_h^{n+1} q_h + a_v(\mathbf{u}_h^{n+1} \cdot \mathbf{n}, \mathbf{v}_h \cdot \mathbf{n}) \\ & + \rho^s \epsilon \int_{\Sigma} \partial_{\tau} \dot{\eta}_h^{n+1} \mathbf{v}_h \cdot \mathbf{n} + a_e(\eta_h^{n+1}, \mathbf{v}_h \cdot \mathbf{n}) = - \int_{\Gamma} p_{\Gamma}(t_{n+1}) \mathbf{v}_h \cdot \mathbf{n} \end{aligned} \quad (5)$$

for all  $(\mathbf{v}_h, q_h) \in \mathbf{V}_h \times Q_h$ . On the other hand, using the definition of  $L_h^e$ , the solid sub-step (4) can be reformulated as

$$\mathbf{u}_h^{n+1} \cdot \mathbf{n}|_{\Sigma} = \dot{\eta}_h^{n+1} + \tau(\rho^s \epsilon)^{-1} L_h^e (\eta_h^{n+1} - \eta_h^*). \quad (6)$$

Therefore, Algorithm 1 corresponds to the implicit time discretization (5), of (2), with the perturbed interface kinematic continuity (6) (instead of  $\mathbf{u}_h^{n+1} \cdot \mathbf{n}|_{\Sigma} = \dot{\eta}_h^{n+1}$ ). This observation, is crucial for the derivation of the stability and consistency results stated in Propositions 3.3 and 3.4 below. Indeed, it suffices to estimate how the perturbation  $\tau(\rho^s \epsilon)^{-1} L_h^e (\eta_h^{n+1} - \eta_h^*)$  affects the stability and the consistency of the underlying implicit coupling scheme.

**Remark 3.2** *Note that it is precisely the perturbation, introduced by (6), what allows the decoupled computation of the fluid  $(\mathbf{u}_h^{n+1}, p_h^{n+1})$  and the solid  $(\eta_h^{n+1}, \dot{\eta}_h^{n+1})$  unknowns, via sub-steps (3) and (4).*

### 3.1 Stability

For  $n \geq 0$ , we define the total discrete energy and dissipation of the fluid-structure system, at time level  $n$ , as

$$\begin{aligned} E_h^n & \stackrel{\text{def}}{=} \frac{\rho^f}{2} \|\mathbf{u}_h^n\|_{0,\Omega^f}^2 + \frac{\rho^s \epsilon}{2} \|\dot{\eta}_h^n\|_{0,\Sigma}^2 + \frac{1}{2} a_e(\eta_h^n, \eta_h^n), \\ D_h^n & \stackrel{\text{def}}{=} \sum_{m=0}^{n-1} \tau \left( 2\mu \|\boldsymbol{\epsilon}(\mathbf{u}_h^{m+1})\|_{0,\Omega^f}^2 + a_v(\dot{\eta}_h^{m+1}, \dot{\eta}_h^{m+1}) \right). \end{aligned}$$

We then have the following energy based stability result, whose proof can be found in the forthcoming work [4]. The symbol  $\lesssim$  indicates an inequality up to a multiplicative constant (independent of the physical and discretization parameters).

**Proposition 3.3** *Assume that  $p_{\Gamma} = 0$  (free system). The following a priori energy estimates hold for  $n \geq 1$ :*

$$E_h^n + D_h^n \lesssim \begin{cases} E_h^0, & \text{if } \eta_h^* = 0, \\ E_h^0 + \tau^2 a_e(\dot{\eta}_h^0, \dot{\eta}_h^0) + \frac{\tau^2}{\rho^s \epsilon} \|L_h^e \eta_h^0\|_{0,\Sigma}^2, & \text{if } \eta_h^* = \eta_h^n, \\ e^{t_n/(\alpha^{-5} - \tau)} E_h^0, & \text{if } \begin{cases} \eta_h^* = 2\eta_h^n - \eta_h^{n-1}, \\ \tau \omega_e^{\frac{6}{5}} \leq \alpha h^{\frac{6}{5}}, \\ \tau < \alpha^{-5}, \end{cases} \end{cases}$$

where  $\omega_e \stackrel{\text{def}}{=} \sqrt{\beta_e/(\rho^s \epsilon)}$  represents a maximum solid elastic-wave speed and  $\alpha > 0$  is the 6/5-CFL constant.

Some remarks are in order. The above proposition shows that the non-incremental displacement-correction scheme,  $\eta_h^* = 0$ , is unconditionally stable in the energy norm. A similar estimate is proved in [7] for this case. The above proposition also shows that the incremental scheme with  $\eta_h^* = \eta_h^n$  is unconditionally stable in the energy norm, *e.g.*, under regularity assumptions on the initial data:  $\eta_0, v_0 \in H^1(\Sigma)$  and  $L^e \eta_0 \in L^2(\Sigma)$ . Indeed, in this case we can chose the initial discrete displacement and velocity  $\eta_h^0, \dot{\eta}_h^0 \in X_h$  as the *a*-*Ritz projections* of  $v_0$  and  $\eta_0$  into  $X_h$  (that is,  $L_h^e \eta_h^0 = L_h^e \eta_0$  and  $L_h^e \dot{\eta}_h^0 = L_h^e v_0$ ), so that  $a_e(\dot{\eta}_h^0, \dot{\eta}_h^0) \leq a_e(v_0, v_0)$  and  $\|L_h^e \eta_h^0\|_{0,\Sigma} \leq \|L^e \eta_0\|_{0,\Sigma}$  (see Remark 3.1). At last, Proposition 3.3 shows that the incremental scheme with  $\eta_h^* = 2\eta_h^n - \eta_h^{n-1}$  is conditionally energy stable, under a 6/5-CFL constraint.

### 3.2 Consistency

The stability estimates provided by Proposition 3.3 can now be used to show how the perturbed constraint (6) influences the precision. This is stated in the next result, whose proof can be found in [4].

**Proposition 3.4** *In the energy-norm, the consistency of the perturbation introduced by (6) rates as:*

- (i)  $\sqrt{\tau/(\rho^s \epsilon)} \|L^e \eta\|_{L^2((0,t_n) \times \Sigma)}$ , if  $\eta_h^* = 0$ ;
- (ii)  $\tau \sqrt{t_n/(\rho^s \epsilon)} \|L^e \partial_t \eta\|_{L^2((0,t_n) \times \Sigma)}$ , if  $\eta_h^* = \eta_h^n$ ;
- (iii)  $\tau^2 \sqrt{e^{t_n/(\alpha^{-5}-\tau)}/(\rho^s \epsilon)} \|L^e \partial_{tt} \eta\|_{L^2((0,t_n) \times \Sigma)}$ , if  $\eta_h^* = 2\eta_h^n - \eta_h^{n-1}$ .

The above result predicts a sub-optimal convergence rate  $\mathcal{O}(\sqrt{\tau})$  for the non-incremental case in the energy-norm, while optimal time accuracy is expected for the incremental schemes given in Algorithm 1.

**Remark 3.5** *It is worth noticing that, a somewhat similar behavior has been observed in pressure error estimates of projection methods for fluids (see, e.g., [6, Section 3]).*

**Remark 3.6** *Note that the constant of the consistency rate introduced by (6) is proportional to  $\beta_e/\sqrt{\rho^s \epsilon}$ .*

## 4 Numerical experiment

In order to illustrate the accuracy of the proposed schemes, we consider a simplified version of the benchmark considered in [7]. We couple the 2D Stokes equations with a 1D generalized string model,  $L^e = c_1 \partial_{xx} + c_0$  and  $L^v = 0$  in (1). The fluid domain is given by the rectangle  $\Omega = [0, 6] \times [0, 0.5]$  and the interface by the segment  $\Sigma = [0, 6] \times \{0.5\}$ , all the space units are in *cm*. At  $x = 0$  we impose a sinusoidal pressure of maximal amplitude  $2 \times 10^4$  *dyne/cm<sup>2</sup>* during  $5 \times 10^{-3}$  *s*, corresponding to half a period. Zero pressure is enforced at  $x = 6$  and a symmetry condition is applied on the lower wall  $y = 0$ . The fluid physical parameters are given by  $\rho^f = 1.0$  *g/cm<sup>3</sup>*,  $\mu = 0.035$  *poise*. For the solid we have  $\rho^s = 1.1$  *g/cm<sup>3</sup>*,  $\epsilon = 0.1$  *cm*,  $c_1 = E\epsilon/(2(1 + \nu))$  and  $c_0 = E\epsilon/(0.25(1 - \nu^2))$ , with Young's modulus  $E = 0.75 \times 10^6$  *dyne/cm<sup>2</sup>* and Poisson's ratio  $\nu = 0.5$ .

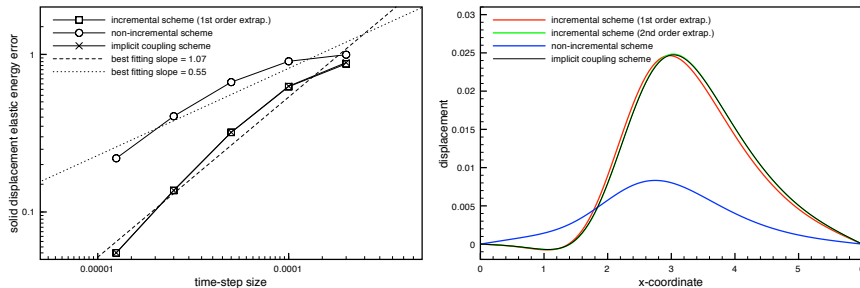


Figure 1: Left: displacement convergence history in time,  $\tau = \mathcal{O}(h)$ . Right: displacement at time  $t = 0.01$  s.

Affine finite elements are used for both the fluid and the structure (a pressure-stabilized formulation is considered in the fluid). All the computations have been performed with FreeFem++ [8]. Figure 1(left) reports the time-convergence history of the solid displacement, in the relative energy-norm at time  $t = 0.01$ , for the incremental ( $\eta_h^* = \eta_h^n$ ), non-incremental and implicit schemes. We have refined both in time and in space ( $\tau = \{2, 1, 0.5, 0.25\} \times 10^{-4}$ ,  $h = 500\tau$ ): this highlights the  $h$ -uniformity of the time-convergence. The reference solution has been generated with the implicit scheme and a high grid resolution:  $\tau = 10^{-6}$  and  $h = 5 \times 10^{-3}$ . The incremental and implicit schemes show an overall  $\mathcal{O}(\tau)$  optimal accuracy, while a sub-optimal overall rate is obtained with the non-incremental scheme. Thus, in agreement with the results of Proposition 3.4. This enhanced accuracy is also clearly highlighted in Figure 1(right), where we show a comparison of the solid displacements at time  $t = 0.01$ , obtained with  $\tau = 10^{-4}$  and  $h = 0.05$ . Note that, in this case, the second-order extrapolation is superfluous since the overall time-accuracy of the underlying implicit scheme is  $\mathcal{O}(\tau)$ .

## 5 Conclusion

We have proposed two incremental displacement correction schemes for the explicit coupling of a thin structure with an incompressible fluid. The resulting coupling schemes can be interpreted as interface kinematic perturbations of an underlying implicit coupling scheme. Their stability properties are independent of the added-mass effect. These schemes yield optimal  $\mathcal{O}(\tau)$  time-accuracy in the energy-norm, while a sub-optimal  $\mathcal{O}(\sqrt{\tau})$  convergence rate is expected for the original non-incremental variant (proposed in [7]). Numerical tests in a benchmark confirm these theoretical results.

## References

- [1] E. Burman and M.A. Fernández. Stabilization of explicit coupling in fluid-structure interaction involving fluid incompressibility. *Comput. Methods Appl. Mech. Engrg.*, 198(5-8):766–784, 2009.

- 
- [2] P. Causin, J.-F. Gerbeau, and F. Nobile. Added-mass effect in the design of partitioned algorithms for fluid-structure problems. *Comput. Methods Appl. Mech. Engrg.*, 194(42–44):4506–4527, 2005.
  - [3] D. Chapelle and K.J. Bathe. *The Finite Element Analysis of Shells - Fundamentals*. Springer, 2003.
  - [4] M.A. Fernández. Incremental displacement-correction schemes for incompressible fluid-structure interaction: stability and convergence analysis. In preparation.
  - [5] L. Formaggia, A. Quarteroni, and A. Veneziani, editors. *Cardiovascular Mathematics. Modeling and simulation of the circulatory system*, volume 1 of *Modeling, Simulation and Applications*. Springer, 2009.
  - [6] J. L. Guermond, P. Minev, and J. Shen. An overview of projection methods for incompressible flows. *Comput. Methods Appl. Mech. Engrg.*, 195(44–47):6011–6045, 2006.
  - [7] G. Guidoboni, R. Glowinski, N. Cavallini, and S. Canic. Stable loosely-coupled-type algorithm for fluid-structure interaction in blood flow. *J. Comp. Phys.*, 228(18):6916–6937, 2009.
  - [8] O. Pironneau, F. Hecht, A. Le Hyaric, and J. Morice. Freefem++, [www.freefem.org/ff++](http://www.freefem.org/ff++).



---

Unité de recherche INRIA Rocquencourt  
Domaine de Voluceau - Rocquencourt - BP 105 - 78153 Le Chesnay Cedex (France)

Unité de recherche INRIA Futurs : Parc Club Orsay Université - ZAC des Vignes  
4, rue Jacques Monod - 91893 ORSAY Cedex (France)

Unité de recherche INRIA Lorraine : LORIA, Technopôle de Nancy-Brabois - Campus scientifique  
615, rue du Jardin Botanique - BP 101 - 54602 Villers-lès-Nancy Cedex (France)

Unité de recherche INRIA Rennes : IRISA, Campus universitaire de Beaulieu - 35042 Rennes Cedex (France)

Unité de recherche INRIA Rhône-Alpes : 655, avenue de l'Europe - 38334 Montbonnot Saint-Ismier (France)

Unité de recherche INRIA Sophia Antipolis : 2004, route des Lucioles - BP 93 - 06902 Sophia Antipolis Cedex (France)

---

Éditeur  
INRIA - Domaine de Voluceau - Rocquencourt, BP 105 - 78153 Le Chesnay Cedex (France)  
<http://www.inria.fr>  
ISSN 0249-6399